Structural, chemical, and magnetic properties of Fe films grown on InAs(100)

L. Ruppel, G. Witte,* and Ch. Wöll
Physikalische Chemie I, Ruhr-Universität Bochum, 44780 Bochum, Germany

T. Last, S. F. Fischer,† and U. Kunze
Werkstoffe und Nanoelektronik, Ruhr-Universität Bochum, 44780 Bochum, Germany
(Received 31 July 2002; published 16 December 2002)

The structure of epitaxial Fe films grown on an InAs(100)-$c(8\times2)/(4\times2)$ surface has been studied *in situ* by means of low-energy electron diffraction and x-ray photoelectron spectroscopy, while their magnetic properties were characterized *ex situ* by superconducting quantum interference device magnetometry at temperatures of 5–300 K. Deposition of iron at room temperature or below leads to the formation of a thin iron arsenide layer that floats on the Fe film upon further deposition. Postdeposition annealing causes no significant improvement of the film structure but activates a further arsenic diffusion through the Fe film. Significant exchange-bias effects were found at low temperatures for insufficiently capped and partially oxidized Fe films, and are attributed to noncollinear spin order at the Ag capping layer/Fe interface. For perfect, nonoxidized Fe films, such a noncollinear spin order at the Fe/InAs interface is excluded as no thermomagnetic irreversibilities were found. This indicates that the spin order at the Fe/InAs interface is suitable for spin injection.

DOI: 10.1103/PhysRevB.66.245307 PACS number(s): 85.75.−d, 75.70.−i

I. INTRODUCTION

The aim of developing magnetoelectronic devices based on spin-dependent transport mechanisms has raised strong interest in the physics of ferromagnetic (FM) metal/nonmagnetic semiconductor (SC) interfaces.[1] On the one hand, easy technological processing, high Curie temperatures, and low coercive fields recommend soft ferromagnetic metals such as permalloy or iron as potential spin-polarizing contacts for room-temperature operation without external magnetic fields. On the other hand, the required high degree of spin manipulation in the transport channel favors InAs as a suitable semiconductor on account of its pronounced Rashba effect.[2,3] Recent studies have shown that in spite of a large lattice mismatch, epitaxial Fe(100) films can be grown on InAs(100) and form ohmic contacts.[4,5] Despite significant effort, however, a spin injection and subsequent detection by the spin blockade, which is the essential element of the spin transistor,[3] has not yet been demonstrated. In addition to an impedance mismatch between semiconductor and metallic contact,[6,7] further limitations of a polarized injection efficiency are expected to arise from spin-flip scattering due to structural and chemical interface roughness or from antiferromagnetic alloys as, e.g., iron arsenide.[8,9] While earlier studies have reported that the growth of Fe films on InAs(100) results in the formation of iron arsenide as well as an indium segregation at the interface,[10,11] the spin alignment at the interface has not yet been examined.

Here we report on a combined low-energy electron-diffraction (LEED) and x-ray photoelectron spectroscopy (XPS) study of the structural and chemical properties of thin epitaxial Fe films grown on InAs(100) and of the Fe/InAs interface with a particular emphasis on alloy formation and its influence on magnetic properties of the films that were characterized by superconducting quantum interference device (SQUID) magnetometry. Conventional high-precision magnetometry is only rarely employed to gain insight into magnetic properties of FM/SC interfaces of interest as it always measures an effective sample magnetization. However, its versatility allowing wide range variations in temperature, field, and sample orientation makes it, however, a valuable tool to investigate the hidden interfaces. In contrast to previous studies on Fe/InAs, where Fe films have frequently been prepared at elevated temperatures while their magnetic properties were studied at room temperature,[4,5,10,12–15] in the present study Fe films were grown at room temperature and their magnetic properties were investigated at temperatures ranging from 5 K to 300 K. Moreover, the influence of the cap layer on the magnetic properties was studied and significant exchange-bias effects were found for insufficient capping, resulting in partial oxidation of the iron film. The SQUID measurements indicate a noncollinear spin order at the capping layer/Fe interface at low temperatures and an enhanced magnetic roughness at room temperature. Such effects are important regarding the domain configuration and magnetization reversal of ferromagnetic electrodes for spin injection in electronic devices.

II. EXPERIMENT

The film growth and sample characterization was carried out in a multitechnique UHV apparatus (base pressure 2×10^{-10} mbar) with a sample load lock system that is described in detail elsewhere.[16] Briefly, this apparatus is equipped with a x-ray photoemission spectrometer consisting of a twin x-ray source (VG XR3E2 with Al and Mg anodes) together with a hemispheric electron energy analyzer (LH EA200, overall resolution 0.9 eV) and a microchannel-plate LEED system (OCI). The epiready InAs(100) wafers (CrysTec) were cut into pieces of 4×5 mm^2 and mounted as twin samples on a variable-temperature sample holder (110–1000 K), yielding an effective film area of 4×3.7 mm^2 on each sample. The InAs samples were prepared by repeated cycles of Ar-ion sputtering (500 eV for 30 min at 575 K) and sub-

sequent annealing at 750 K. After 3–5 cycles, no traces of contaminations were found in the corresponding XP spectra within the detection limit of about 2% of a monolayer and a sharp LEED pattern of the $c(8\times2)/(4\times2)$ phase with a low background signal was observed. Iron and silver were deposited from a molecular-beam epitaxy source (Omicron, EFM3T) at room temperature with typical growth rates of about 1.3–1.5 Å/min. The deposition rates were monitored by a quartz microbalance (Inficon, XTM2) that had been cross calibrated by XPS and atomic force microscopy (AFM) measurements on evaporated mesa structures, yielding an accuracy of the given film thickness of about 5%. The magnetic properties of the films were characterized with a SQUID magnetometer (quantum design, MPMS 5) allowing measurements at variable temperatures between 5 and 300 K. All hysteresis loops were corrected for the diamagnetic contributions from the substrate and from the sample holder.

III. RESULTS

A. Growth and structure of Fe films

In the present study, all Fe films have been grown on the indium-rich $c(8\times2)/(4\times2)$ reconstructed InAs(100) surface to provide a reproducible substrate with a well-known microstructure.[17–19] As demonstrated in previous studies by Bland and co-workers, epitaxial Fe films can be grown on that substrate.[4,5,12] It is believed that the arsenic impoverishment of this surface phase minimizes a possible formation of iron arsenide. After standard preparation (described in Sec. II), a distinct LEED pattern was obtained for the clean substrate revealing a mixture of (4×2) and $c(8\times2)$ structures. Occasionally, it was possible to observe a pure $c(8\times2)$ phase where all diffraction spots along the $[01\bar{1}]$ direction could be well separated in the corresponding LEED pattern, as shown in Fig. 1(a).

During initial iron deposition at room temperature, the LEED pattern became faint and an intermediate (4×1) structure appeared at a nominal Fe layer thickness of about 0.1 nm.[20] Further deposition led to a disappearance of the diffraction spots. When again increasing the film thickness above 1.5 nm, broad diffraction spots reappeared, which sharpened up upon further deposition until at thicknesses of about 2.5 nm a distinct Fe(100)-(1×1) LEED pattern developed [see Fig. 1(b)]. The quantitative analysis of the LEED pattern yields a lattice constant of 2.9 ± 0.15 Å, in close agreement with the Fe bulk value of $a=2.866$ Å without any noticeable azimuthal anisotropy. The comparison of both LEED patterns shown in Fig. 1 confirms the epitaxial relationship between substrate and film, Fe(100)[010]‖InAs(100)[010], which has been observed before by Xu *et al.*[4,5] The LEED pattern of the films did not improve significantly upon annealing after deposition. However, such annealing causes an enhanced interface diffusion (as shown in the following), so that all Fe films have been prepared at room temperature.

The chemical composition of the films and the interface was monitored by XPS measurements for various Fe layer thicknesses. In order to provide an accurate energy calibration, all binding energies have been referenced to a Au-4$f_{7/2}$ binding energy[21] of 83.8 eV, which was measured additionally for a gold foil mounted next to the InAs wafers on the sample holder. Figure 2(a) shows the evolution of the As-3*d* region with increasing Fe film thickness. In addition to the As-3*d* peak at $E_B=41.2$ eV, which is strongly attenuated with increasing Fe film thickness, a second peak appears at 42.7 eV. The corresponding peak intensities were determined by fitting a Gaussian to the experimental data after a linear background subtraction and subsequent integration of the peak areas. As depicted in Fig. 2(d), the intensity of this new peak remains almost constant, whereas the intensity of the substrate-related As-3*d* peak decreases almost exponentially with increasing film thickness. In a previous study on GaAs, Sorba *et al.* have identified the presence of a surface-related arsenic species on the basis of high-resolution XPS measurements,[22] which is characterized by a reduced binding energy of about 0.4 eV with respect to the As-3*d* line of the bulk species. Such a substrate surface-related feature, however, cannot account for the As-3*d* line seen here because it was not found for the clean InAs surface, and moreover, its intensity does not decrease upon iron deposition. On the other hand, metallic arsenic is also unlikely to be the origin since its As-3*d* binding energy amounts to 41.4 eV, which is very close to that of the InAs substrate.[23] Instead, we attribute this new peak to an iron arsenide species (Fe_xAs_y). This assignment is corroborated by recent high-resolution XPS measurements on $FeAs_2$ (Loellingite), where in addition to a bulk-related species with a As-3*d* binding energy of 41 eV, a further, surface-related species at $E_B=42$ eV was found.[24] The same signature, namely, the appearance of an additional As-3*d* peak shifted by 1.4 eV towards higher

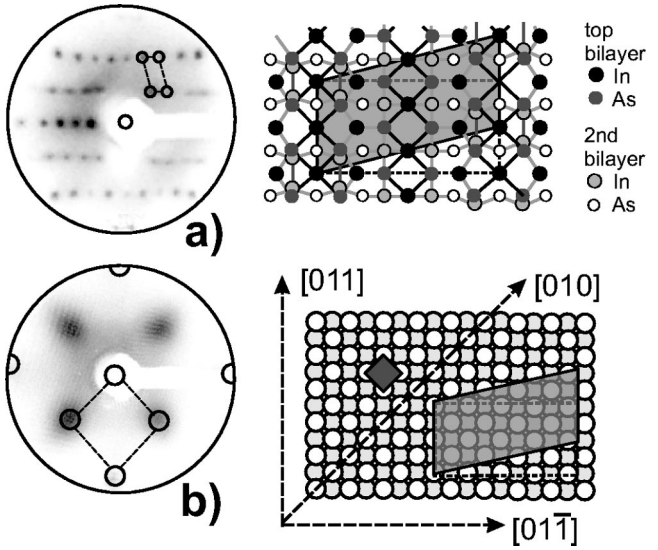

FIG. 1. LEED pattern of (a) the clean InAs(100)-c(8×2) substrate taken at $E=80$ eV and (b) after growth of a 12-nm Fe film ($E=100$ eV) together with corresponding hard-sphere models of the reconstructed InAs surface (as suggested in Ref. 17) and the Fe(100) film. Note, that the slight image distortion is caused by the plane multichannel plates of the LEED system. The dashed or dark parallelograms represent the unit cells of the film and the underlying substrate.

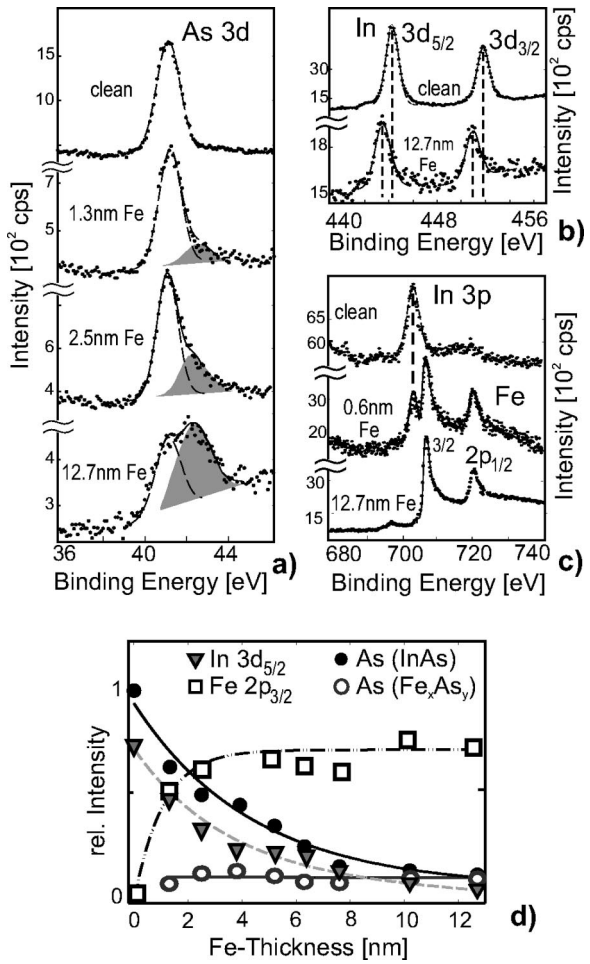

FIG. 2. Summary of XPS data obtained for the clean InAs substrate and thin epitaxially grown Fe films recorded for a photon energy of 1486.6 eV (Al K_α). Panels (a–c) show high-resolution photoelectron spectra of (a) the As-3d region, (b) the In-3d doublet, and (c) the In-3p region and the Fe-2p doublet, respectively. The additional As-3d state appearing upon Fe deposition (marked as a gray peak) is attributed to an iron arsenide species. The relative core-level intensities are summarized in panel (d) as a function of the Fe film thickness.

binding energies after deposition of 10-ML Fe (where ML stands for monolayer) on InAs(100) was also reported by Teodorescu *et al.*[14] The fact that the intensity of the As-3d line at 41.2 eV reveals an almost exponentiell attenuation, whereas the line at 42.7 eV assigned to iron arsenide stays nearly constant, corroborates the finding that iron arsenide floats on top of the Fe layer.

Figure 2(b) displays the In-3d doublet of the clean substrate and after deposition of a 12.7-nm Fe film. In addition to the peak attenuation through the iron film, a continuous shift of the In-3$d_{5/2}$ binding energy from 443.5 eV for the clean surface to about 442.7 eV for a 12.7-nm Fe film was observed. Furthermore, the In-3p region is shown in Fig. 2(c), which is superimposed and finally dominated by the Fe-2p doublet. The evolution of the intensities obtained for the different core levels is summarized in Fig. 2(d) as a function of the Fe thickness.

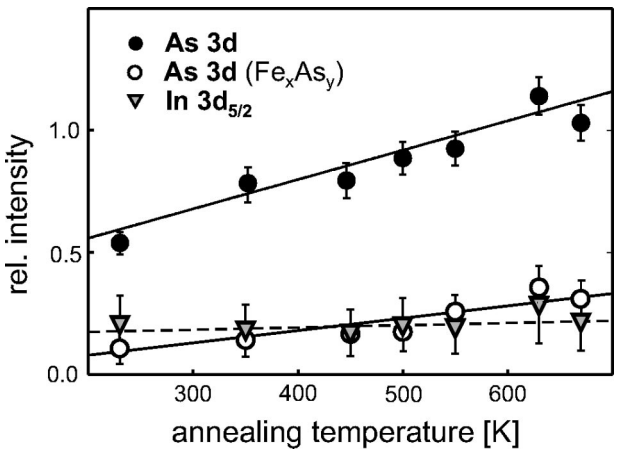

FIG. 3. Evolution of different core-level intensities obtained for a 3.9-nm Fe film grown at 230 K upon subsequent annealing.

To study further the influence of annealing on the chemical composition, a 3.9-nm Fe film was grown at low temperature (230 K). Subsequently, the film was heated to different temperatures for 1 min before cooling back to room temperature and recording the XP spectra. The resulting peak intensities are summarized in Fig. 3. Evidently, a clear increase in the arsenic signal can be seen, whereas the indium signal remains almost constant and thus reflects a thermal activated diffusion of the more volatile arsenic. Compared with arsenic, the intensity of the arsenide species reveals only a small increase with increasing annealing temperature.

B. Magnetic properties

In order to allow for *ex situ* magnetic characterization of the Fe films by SQUID magnetometry, a protection against oxidation was required. To this end, the Fe layers were covered by thick silver film of about 21 nm deposited at room temperature before removal from the vacuum. The Ag cap layer was found to grow epitaxially with (100) orientation as seen in the corresponding LEED patterns. Moreover, XPS measurements revealed no traces of As or Fe, thus indicating a high quality of the cap layers. To check whether such cap layers provide a complete oxidation protection, the films were also analyzed by XPS after the SQUID measurements. The XPS data obtained after partial removal of the cap layer by sputtering clearly showed the clean iron film without any traces of oxygen or iron oxide, and thus confirmed a proper protection.

Figure 4 displays the typical ferromagnetic behavior of a 3.9-nm Fe film on InAs(100) at room temperature and at 5 K. The magnetic field was applied in-plane along the $[01\bar{1}]$, [010], and [011] substrate axis revealing an in-plane anisotropy. At 300 K, coercive fields of 1 Oe and less were found along the $[01\bar{1}]$ and [010] directions, while an enhanced coercive field H_c of 9 Oe and an increased saturation field were measured along [011], indicating the magnetic hard axis. Noncollinear spin alignment, for example, at the interface was checked by cooling the sample from 300 K to 5 K in an applied field of $+2500$ Oe (i.e., larger than the saturation fields at 300 K). Magnetic materials or layered systems in-

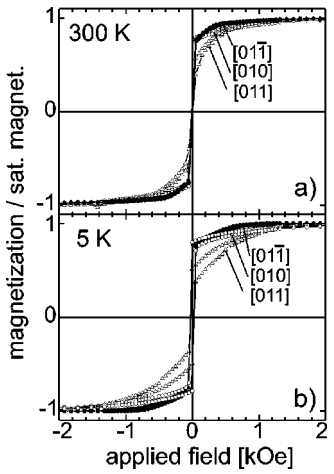

FIG. 4. Magnetic hysteresis loops of an epitaxial 3.9-nm Fe film ($\approx$27 ML) on InAs(100) capped with 21-nm Ag measured along different in-plane axes at (a) 300 K and after cooling in an applied field of +2500 Oe at (b) 5 K.

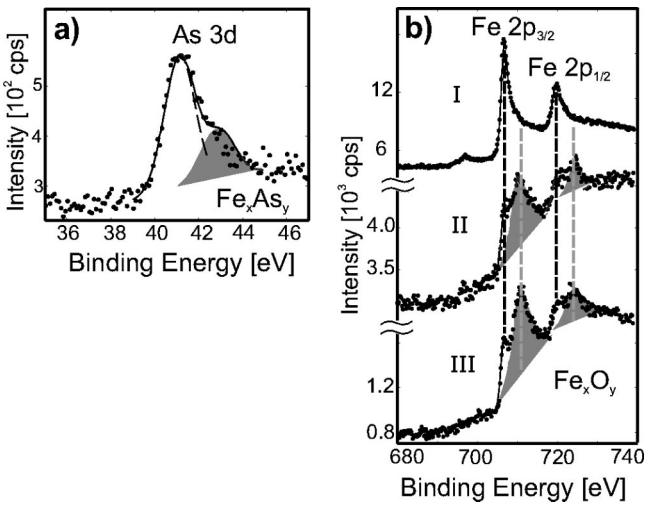

FIG. 5. (a) XP spectra of the As-3*d* region measured for a 3.9-nm Fe film covered by a 1-nm Ag layer. (b) Series of XP spectra of the Fe-2*p* doublet recorded for (i) a 3.9-nm Fe film directly after capping with a 1-nm Ag layer and (ii) after the SQUID measurements. For comparison, a corresponding spectrum of an oxidized Fe surface is shown in (iii).

corporating antiferromagnetic-ferromagnetic coupling often show irreversible thermomagnetic behavior, such as strongly increased coercive fields or a hysteresis asymmetry after cooling in applied magnetic fields. None of these thermomagnetic irreversibilites were found for the present Fe/InAs(100) samples with 21-nm Ag capping layer as shown in Fig. 4(b). Coercive fields only slightly increase to 25 Oe along the [01$\bar{1}$] and [010] substrate axis and to 29 Oe along the [011] azimuth direction. The magnetic moment can be estimated from the saturation magnetization at 5 K and yields a value of about 1.2×10^3 emu/cm^3, which is distinctively reduced compared to the magnetic moment of the bulk bcc iron (1.7×10^3 emu/cm^3). However, we attribute this reduction only partially to the existence of an iron arsenide layer that gives rise to a reduced effective Fe layer thickness since a precise analysis was hampered by experimental uncertainties in the absolute magnetization values of about 20%.

C. Partial oxidation

The influence of an insufficient capping on the magnetic properties of the films was further studied by additional measurements of a 3.9-nm Fe film covered with only 1 nm of Ag. The high transparency for photoelectrons of such thin cap layers allowed also detailed XPS measurements through the Ag film, that was utilized to demonstrate that the iron arsenide species still remains underneath the Ag film [see Fig. 5(a)]. XPS measurements recorded after exposing the sample to air for about 12 h clearly showed the presence of an additional Fe-2*p* doublet revealing the presence of iron oxide. This assignment was confirmed by XPS data obtained for a specifically oxidized iron film without any cap layer, which is also shown for comparison in Fig. 5(b).

The magnetic properties of partially oxidized Fe films on InAs were characterized by hysteresis loops taken with an applied field along the [01$\bar{1}$] film axis. At first, measurements were carried out at room temperature [Fig. 6(f)], then the sample was cooled down to 5 K in an applied field of +350 Oe (i.e., larger than the saturation field at 300 K), and the hysteresis loop was measured at 5 K [Fig. 6(a)]. Subsequently, a series of hysteresis loops were recorded for increasing temperatures up to 300 K, some of which are shown in Figs. 6(a–f). In contrast to the pure Fe/InAs adlayers, the partially oxidized film exhibits at low temperatures a pronounced asymmetry of the hysteresis loops with respect to the zero-field axis. In the following, the field shift away from the zero-field axis is denoted as exchange bias H_e.

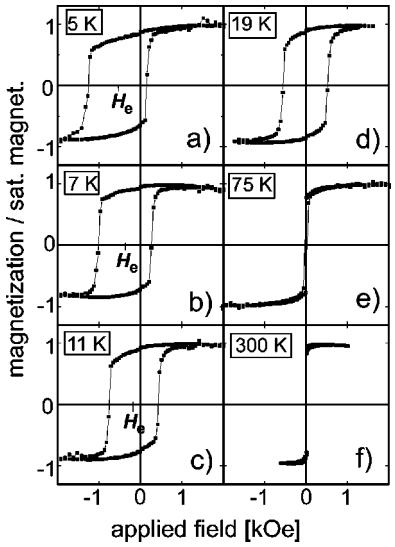

FIG. 6. Magnetic hysteresis loops of an epitaxial 3.9-nm Fe film on InAs(100) covered by 1-nm Ag. After cooling from 300 K to 5 K in an applied in-plane field of +350 Oe (along [01$\bar{1}$]), the measurements were taken subsequently with increasing temperature, (a–f).

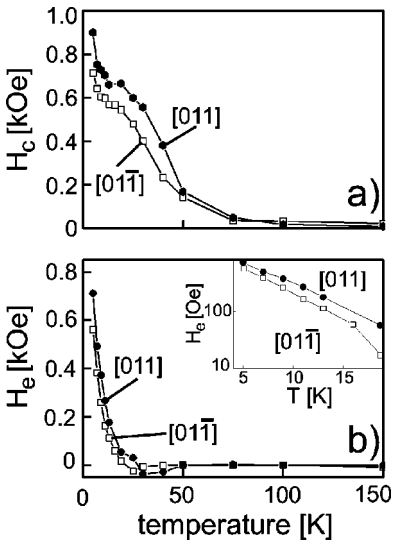

FIG. 7. Temperature dependence of (a) the coercive field H_c and (b) the exchange bias field H_e of epitaxial Ag (1 nm)/Fe (3.8 nm)/InAs(100) measured from 5 K to 300 K after cooling in an applied field of $+350$ Oe from 300 K to 5 K. The inset of (b) shows the data on a logarithmic scale.

With increasing temperature, the exchange bias H_e as well as the asymmetry in the hysteresis shape decrease [see Figs. 6(a–d)] and disappear at about 30 K, while the coercive field H_c vanishes at a temperature of about 150 K. The detailed temperature dependence of H_c and H_e are given in Figs. 7(a) and 7(b), respectively.

In Fig. 8, magnetic hysteresis loops measured at 5 K after cooling in differently in-plane oriented applied fields are shown. While $H_e(T)$ is nearly independent of the cooling field orientation with respect to film crystal axes $H_c(T)$ and the shape of hysteresis exhibits an in-plane anisotropy [cf. Figs. 8(a,b)]. Hysteresis loops taken after cooling in applied

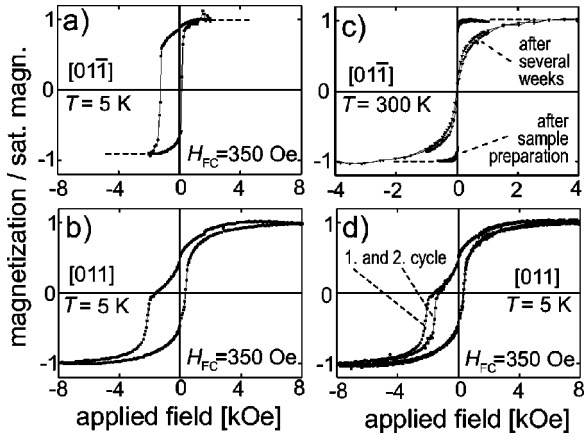

FIG. 8. Magnetic hysteresis loops of a 3.9-nm Fe film on InAs(100) capped by 1-nm Ag. (a) Measured at 5 K after cooling in an applied in-plane field ($+350$ Oe) along the [01$\bar{1}$] direction and (b) along the [011] direction. (c) Measured at 300 K directly after sample fabrication and several weeks later (sample ageing). (d) Training effect: comparison of magnetic hysteresis loops measured as in (b) for the 1 and 2 hysteresis cycles.

fields along the magnetic hard axis [011] show a hysteresis asymmetry not only as a shift on the field axis but also in hysteresis shape. Concerning several warming and cooling cycles, a training effect of the magnetic field for zero magnetization (negative field axis) was found at 5 K, as shown in Fig. 8(d). Further measurements that were carried out several weeks later reveal a significant change in the shape of the hysteresis loop [see Fig. 8(c)], which indicates an ongoing ageing, i.e., oxidation of the sample.

IV. DISCUSSION

A. Film structure

The results of the present study confirm earlier findings in that ordered epitaxial Fe(100) films can be grown on InAs(100) at room temperature. The observed gradual disappearance of the substrate LEED pattern during the early stage of iron deposition reflects the initial island growth before continuous films are formed, which has also been observed directly by scanning tunneling microscopy (STM).[4,12] The remaining finite spot size of the LEED pattern observed also for Fe layer thicknesses of more than 10 nm indicates, however, a somewhat granular structure of the deposited Fe films.

Corresponding XPS data recorded immediately after initial iron deposition reveal the appearance of a new arsenide species with a characteristic As-3d binding energy shifted by about $+1.5$ eV compared to the clean InAs. This new peak is assigned to iron arsenide (Fe_xAs_y). While the intensity of the InAs As-3d peak decreased with increasing Fe film thickness, the Fe_xAs_y As-3d line revealed an almost constant intensity. This is an important observation that strongly indicates that the iron arsenide layer is floating on top of the Fe film. Considering their relative atomic sensitivities[21,25] and a mean free path of about $\lambda = 13.6$ Å for the Fe-2p photoelectrons,[26] the quantitative analysis of the relative intensities of As-3d and Fe-2p lines obtained for a 12-nm-thick Fe film yields an effective thickness for the iron arsenide layer of about 2.3 Å (corresponding to 1.6 ML). The fact that despite the presence of this additional surface arsenide a distinct Fe(100) LEED pattern was observed, suggests that iron arsenide is present in form of islands. The formation of iron arsenide was also observed upon iron deposition at low temperatures of 230 K. This is not surprising if one takes into account the kinetic energy of the impinging Fe atoms released from the hot evaporator source.

The present observation of a surface-related iron arsenide layer and its effective thickness is in close agreement with the findings of a previous study by Teodurescu *et al.*[10] We note that their conclusion, however, was solely based on the difference in the attenuation of the indium and arsenide core-level intensities through the Fe film while they did not distinguish in their analysis between iron arsenide and arsenic released from the InAs substrate. This is, however, of relevance as demonstrated by our temperature-dependent XPS measurements that revealed in addition to a slightly increasing iron arsenide signal a pronounced increase of the main As-3d signal with increasing annealing temperature (shown in Fig. 3). Generally, the main As-3d signal at E_B

$=41.2$ eV can originate either from the InAs substrate or from released metallic arsenic that has almost the same binding energy. In the first case, the observed intensity increase would imply a change in the Fe film topography upon heating, such as the formation of islands that effectively reduce the attenuation of the substrate photoelectrons. However, this can be effectively ruled out since at the same time the indium signal of the substrate remains nearly constant, and thus rather suggests a thermally activated diffusion of the volatile As from the substrate to the Fe film surface. Such a diffusion through the Fe film is presumably made possible by its granular structure, of which grain boundaries provide effective diffusion channels.

As regards the indium in addition to an almost exponential intensity decrease, a small shift in the In-3*d* core level of about 0.8 eV towards smaller binding energies was observed in the XPS measurements upon iron deposition. The low intensity, however, did not allow for a more quantitative peak analysis such as a peak decomposition. A similar shift has been reported by Schieffer *et al.* for the In-4*d* level[11] that was studied by ultraviolet photoemission spectroscopy. Initially, they observed a small increase of the In-4*d* binding energy of about 0.1 eV for submonolayer iron coverage, which they attributed to a band bending at the substrate surface. Upon further deposition, they measured a continuous reduction of the binding energy for this level, which amounted to about 0.5 eV for a 32-ML Fe film. According to Schieffer *et al.* this shift is caused by indium atoms that are segregated or dissolved in the Fe film. Whereas generally such peak shifts on metal/semiconductor interfaces can also be caused by changes in the corresponding Fermi level or the local work function, similar effects were not observed for the core levels of arsenic or iron, and hence support the above interpretation. It should also be noted that Teodorescu *et al.* did not observe such a peak shift for the In-3*d* level in their growth study.[10] This might be explained by small variations of the indium concentration of the InAs surface, which depends very critically on the actual preparation since indium tends to form metallic clusters at the surface.

In summary, the formation of a surface-related iron arsenide species in combination with the arsenic impoverishment of the $c(8\times2)/(4\times2)$-reconstructed InAs(100) surface lead to the conclusion that the Fe films actually form an In/Fe interface. Taking further into account that the first iron layers have a granular structure, a certain amount of segregation is not unlikely.

B. Magnetic properties

The measured ferromagnetic behavior of nonoxidized thin epitaxial Fe films on InAs(100) at room temperature presented here compare well with those of other works.[4,5,12,13,15] In view of a possible noncollinear spin structure at the Fe/InAs interface, our work includes additionally studies on thermomagnetic irreversibilities by recording also low-temperature magnetic hysteresis after cooling in an applied field. No thermomagnetic irreversibilities such as hysteresis asymmetry were found for Fe films that were effectively protected against oxidation by thick Ag cap layers. Hence, it appears that for nonoxidized epitaxial Fe films on InAs, noncollinear magnetic coupling does not exist at the Fe/InAs and the Fe/Ag interfaces. Accordingly, this finding is supported by the results of a chemical analysis where no signature of an Fe-As phase at the ferromagnet-semiconductor interface is found which could incorporate antiferromagnetic spin structure unfavorable for spin injection (cf. antiferromagnetic bulk Fe_2As with $T_N\approx353$ K).[27] Thus, based on these magnetometric results together with the outcome of the UHV growth studies, we find no objections against the Fe/InAs heterostructure for spin electronic ferromagnet-semiconductor devices.

For spin electronic applications, microscale or even nanoscale patterning of suitable heterostructures plays a major role.[28] Therefore we investigated further the influence of capping layers that protect Fe/InAs films only partially against oxidation. At the edges of Fe microstructures or nanostructures where the capping layer might be missing or reduced in thickness, a non-negligible influence on the magnetic properties is to be expected by partial oxidation especially for *nanoscale* devices. On the basis of our chemical analysis (Fig. 5) proving partial oxidation of an epitaxial Fe film on InAs, we attribute the observed exchange-bias effects in magnetic hysteresis to antiferromagnetic and/or ferrimagnetic Fe-O phases, such as FeO, Fe_2O_3, or Fe_3O_4. This conclusion is supported by the finding of purely ferromagnetic behavior of nonoxidized Fe films [Fig. 4(b)].

Normally, when a conventional antiferromagnetic (AF)–ferromagnetic (FM) bilayer is cooled below the AF Néel temperature, T_N in the presence of a magnetic field larger than the saturation field of the ferromagnet, the interfacial interactions between the two materials will induce an unidirectional exchange anisotropy that shifts the magnetic hysteresis loops of the ferromagnet away from the zero-field axis.[29–31] The magnitude of this displacement is usually referred to as the exchange bias H_e, which can be defined as $-(H_{\text{left}}+H_{\text{right}})/2$, where H_{left} and H_{right} are the external fields at zero magnetization. In addition to the shift of the hysteresis loop, the coercivity $H_c=-(H_{\text{left}}-H_{\text{right}})/2$ is always found to be enhanced compared to that of a single FM layer. In an extended exchange-biased FM film, the magnetization reversal is mainly controlled by the interfacial exchange coupling between the AF and FM layers. The interfacial exchange anisotropy energy per unit area is commonly given by $\sigma=H_eM_st$ (cf. Ref. 31, and references therein), where M_s denotes the saturation magnetization and t the film thickness of the FM layer. With $M_s=1.2\times10^3$ emu/cm^3, $t=3.9$ nm, and the extrapolated value of H_e (5 K) ≈700 Oe, this relation yields σ (5 K) ≈0.33 erg/cm^2, which corresponds to reported orders of magnitude (0.01–3.5 erg/cm^2) for many AF/FM systems.[31] The blocking temperature T_B below which an exchange bias occurs, must not necessarily coincide with but gives a lower limit of T_N.[31]

Apparently, two different mechanisms contribute to the temperature dependence of the coercive field $H_c(T)$, one of which incorporating a maximum of $H_c(T)$ at about 30 K and

the other showing an exponential decrease. The anticipated maximum of $H_c(T)$ at 30 K coincides with the disappearance of the exchange-bias field. Such behavior is often observed for FM/AF bilayers for temperatures at and below T_B, and is thought to provide important information on the fundamental origin of the exchange bias (cf. Refs. 31,32, and references therein). An exponential decrease of $H_c(T)$ finds an explanation in increased domain-wall mobility by thermal activation.

The temperature dependence of the exchange bias $H_e(T)$ presented on a log-linear scale [cf. inset of Fig. 7(b)] implies an exponential decrease, as possible for an ensemble of AF clusters with a cluster size distribution whose magnetic ordering will decrease by thermal activation. Training effects are indicative of domain formation and domain-wall pinning in the AF phase [Fig. 8(d)]. The hysteresis loops taken after cooling in applied fields along the magnetic hard axis [011] show a hysteresis asymmetry not only as a shift on the field axis but also in hysteresis shape [Fig. 8(b)], which rather implies two mechanisms taking part in magnetization reversal. This is mainly accounted to the ongoing oxidation [Fig. 8(c)] that affects all measurements but the first ones (cf. Fig. 6).

The observed effects of partially oxidized thin epitaxial Fe films have a direct bearing on the magnetization reversal in nanoscale patterned Fe layers with a lateral size below 0.5 μm, as regarded preferably for single-domain contacts. Exchange-bias effects due to insufficient capping are discussed to influence the magnetization reversal in the sense that it is not anymore governed by coherent rotation.[33] Furthermore, coercive fields are increased, domain-wall pinning at the FM/AF interface can contribute to anisotropic magnetoresistance, and an increased number of domain walls is expected to decrease the signal-to-noise ratio in magnetotransport measurements.

V. CONCLUSIONS

In summary, structural and chemical properties of epitaxial Fe(100) films grown on InAs(100) were characterized and correlated with their magnetic properties obtained by variable-temperature *ex situ* SQUID measurements. The initial deposition of iron leads to the formation of a thin iron arsenide layer that stays at the surface also after additional Fe deposition. Corresponding SQUID measurements have shown that such an arsenide film on top of the iron film does not affect the overall ferromagnetic behavior, which indicates a collinear spin ordering at the substrate interface, from which we may infer that the spin order at the interface is suitable for spin electronic devices. Moreover, the present study points out the importance of a complete capping of the Fe/InAs interface since partial oxidation causes magnetic pinning on the upper surface of the ferromagnetic contact electrode that introduces an exchange bias and strongly modifies the magnetic properties.

Finally, we note that similar to Fe/InAs, the magnetic properties of Fe/GaAs were extensively investigated at room temperature,[9,34] but little is known about the low-temperature behavior that could provide further insight into the spin structure at the interface. Low-temperature magnetization measurements after field cooling could be employed here also as a sensitive tool in search for noncollinear magnetic coupling due to interfacial mixing.

ACKNOWLEDGMENTS

This work was supported by the Deutsche Forschungsgemeinschaft (SFB491, TP A3 and B2). The use of the SQUID magetometer provided through the SFB491 is acknowledged. The authors are also grateful to Professor R. Szargan (University Leipzig) for providing XPS data on iron arsenide prior to publication.

*Electronic address: witte@pc.ruhr-uni-bochum.de

†Electronic address: saskia.fischer@ruhr-uni-bochum.de

[1] S.A. Wolf, D.D. Awshalom, R.A. Buhrmann, J.M. Daughton, S. von Molnar, M.L. Roukes, A.Y. Chtchelkanova, and D.M. Treger, Science **294**, 1488 (2001).

[2] Y.A. Bychkov and E.I. Rashba, J. Phys. C **17**, 6039 (1984).

[3] S. Datta and B. Das, Appl. Phys. Lett. **56**, 665 (1990).

[4] Y.B. Xu, E.T.M. Kernohan, M. Tselepi, J.A.C. Bland, and S. Holmes, Appl. Phys. Lett. **73**, 399 (1998).

[5] Y.B. Xu, D.J. Freeland, M. Tselepi, and J.A.C. Bland, Phys. Rev. B **62**, 1167 (2000).

[6] G. Schmidt, D. Ferrand, L.W. Molenkamp, A.T. Filip, and B.J. van Wees, Phys. Rev. B **62**, 4790 (2000).

[7] R.P. Borges, C.L. Dennis, J.F. Gregg, E. Jouguelet, K. Ounadjela, I. Petej, S.M. Thompson, and M.J. Thornton, J. Phys. D **35**, 186 (2002).

[8] M. Zwölfl, M. Brockmann, M. Köhler, S. Kreuzer, T. Schweinbröck, S. Miethaner, F. Bench, and G. Bayreuther, J. Magn. Magn. Mater. **175**, 16 (1997).

[9] F. Bensch, G. Garreau, R. Moosbühler, G. Bayreuther, and E. Beaurepaire, J. Appl. Phys. **89**, 7133 (2001).

[10] C.M. Teodorescu, F. Chevrier, C. Richter, V. Ilakovac, O. Heckmann, L. Lechevalier, R. Brochier, R.L. Johnson, and K. Hricovini, Appl. Surf. Sci. **166**, 137 (2000).

[11] P. Schieffer, B. Lepine, and G. Jezequel, Surf. Sci. **497**, 341 (2002).

[12] M. Tselepi, Y.B. Xu, D.J. Freeland, T.A. Moore, and J.A.C. Bland, J. Magn. Magn. Mater. **226**, 1585 (2001).

[13] T.A. Moore, J. Rothman, Y.B. Xu, and J.A.C. Bland, J. Appl. Phys. **89**, 7018 (2001).

[14] C.M. Teodorescu, F. Chevrier, R. Brochier, C. Richter, O. Heckmann, V. Ilakovac, P. De Padova, and K. Hricovini, Surf. Sci. **482**, 1004 (2001).

[15] J.A.C. Bland, A. Hirokata, C.M. Guertler, Y.B. Xu, and M. Tselepi, J. Appl. Phys. **89**, 6901 (2001).

[16] G. Loepp, S. Vollmer, G. Witte, and Ch. Wöll, Langmuir **15**, 3767 (1999).

[17] C. Kumpf, L.D. Marks, D. Ellis, D. Smilgies, E. Landemark, M. Nielsen, R. Feidenhansl, J. Zegenhagen, O. Bunk, J.H. Zeysing, Y. Su, and R.L. Johnson, Phys. Rev. Lett. **86**, 3586 (2001).

[18] C. Kendrick, G. Lelay, and A. Kahn, Phys. Rev. B **54**, 17 877 (1996).

[19] C. Kendrick, G. Lelay, and A. Kahn, Surf. Rev. Lett. **5**, 229 (1998).

[20] Throughout this paper the film thickness is given in nanometers. Under the assumption that the iron films crystallize in a perfect bcc lattice with a Fe(100) plane separation of 1.433 Å, a given film thickness corresponds to the number of monolayers according to 1 nm≅7 ML.
[21] C.D. Wagner, W.M. Riggs, L.E. Davis, and J.F. Moulder, in *Handbook of X-ray Photoelectron Spectroscopy*, edited by G.E. Muillenberg (Perkin Elmer Corporation, Eden Prairie, MN, 1979).
[22] L. Sorba, M. Pedio, S. Nannarone, S. Chang, A. Raisanen, A. Wall, P. Philip, and A. Franciosi, Phys. Rev. B **41**, 1100 (1990).
[23] N. Martensson, B. Reihl, and O. Vogt, Phys. Rev. B **25**, 824 (1982).
[24] H.W. Nesbitt, I. Uhlig, and R. Szargan, Am. Mineral. **87**, 1000 (2002).
[25] J.H. Scofield, J. Electron Spectrosc. Relat. Phenom. **8**, 129 (1979).
[26] S. Tanuma, C.J. Powell, and D.R. Penn, Surf. Interface Anal. **11**, 577 (1988).
[27] M. Yusumi, R. Taharo, and Y. Nakamura, J. Phys. Soc. Jpn. **48**, 1937 (1980).
[28] H. Ohno, K. Yoh, T. Doi, A. Subagyo, K. Sueoka, and K. Mukasa, J. Vac. Sci. Technol. B **19**, 2280 (2001).
[29] W.H. Meiklejohn and C.P. Bean, Phys. Rev. **102**, 1413 (1956).
[30] W.H. Meiklejohn and C.P. Bean, Phys. Rev. **105**, 904 (1957).
[31] J. Nogues and I.K. Schuller, J. Magn. Magn. Mater. **192**, 203 (1999).
[32] C. Leighton, M.R. Fitzsimmons, A. Hoffmann, J. Dura, C.F. Majkrzak, M.S. Lund, and I.K. Schuller, Phys. Rev. B **65**, 064403 (2002).
[33] S. Zhang and Z. Li, Phys. Rev. B **65**, 054406 (2001).
[34] Y.B. Xu, M. Tselepi, C.M. Guertler, C.A.F. Vaz, G. Wastlbauer, J.A.C. Bland, E. Dudzik, and G. van der Laan, J. Appl. Phys. **89**, 7156 (2001).